Optimal design of a novel remote center-of-motion mechanism for minimally invasive surgical robot

2017 IOP Conf. Ser.: Earth Environ. Sci. 69 012097

(http://iopscience.iop.org/1755-1315/69/1/012097)

IOP Conf. Series: Earth and Environmental Science **69** (2017) 012097 doi:10.1088/1755-1315/69/1/012097

Optimal design of a novel remote center-of-motion mechanism for minimally invasive surgical robot

Jingyuan Sun*, Zhiyuan Yan and Zhijiang Du

State Key Laboratry of Robotics and System, Harbin Institute of Technology, Harbin, 150001, China

*Corresponding author: jingyuan713@outlook.com

Abstract. Surgical robot with a remote center-of-motion (RCM) plays an important role in minimally invasive surgery (MIS) field. To make the mechanism has high flexibility and meet the demand of movements during processing of operation, an optimized RCM mechanism is proposed in this paper. Then, the kinematic performance and workspace are analyzed. Finally, a new optimization objective function is built by using the condition number index and the workspace index.

1 Introduction

In effective health care, basic science, engineering and medical collaborative effort provides physicians with improved tools and technologies. Minimally Invasive Surgery (MIS) has been thoroughly reform the ways of the surgical treatment, and in the progress of surgical robots, again to overhaul the MIS [1]. Bring in surgical robots to the operating room, reduces the trauma and short the recovery time. During the process of a long-time operation, the doctor's fatigue value is small. Especially in the movement of the flexibility, surgical instruments are placed in the tip of the manipulator, which can provide a full range of mobility

Due to the limitation of the incision, surgical instruments need move around a fixed point at the end, which is called remote center-of-motion (RCM) [2]. RCM plays an important role in MIS by avoiding additional trauma except the incision. The request of the numbers of the DOFs is four, including two rotational motions around the incision shown in Figure 1, one spin motion around the instrument axial direction, and one transition along the instrument. For safety, all rotation must be centered on incision, while the translational motion should always move along the line via the incision point.

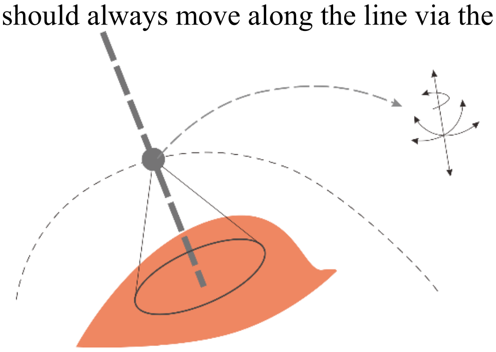

Figure 1: Remote Center of Motion (RCM)

Typical structures of RCM contain parallelogram mechanism, multi-axis linkage, cambered mechanism, spherical, etc. The da Vinci uses double parallelogram mechanism in minimally invasive surgery, which is the most widely used [3]. Tianjin University developed a new type of parallelogram structure. The main characteristic of this structure is that the two axis of the rotation locate in two moving planes respectively, forming a unique intersection, which makes their cross curve always pass through the fixed point.

Many scholars have been working on perfecting a kinematic evaluation index. Gupta analyzed the workspace and selected it as the design principle. Gosselin and Angeles presented a global conditioning (GCI) index [4]. Yoshikawa proposed one method to measure the manipulating ability of the robotic mechanisms in positioning and orienting end effectors [5,6]. Klein suggested that the workspace quality could be measured by a single value [7]. Stocco[8] presented a new technique to cope with the problem of nonhomogeneous physical units.

Lan proposed a performance index combined the mechanism speed and dexterity, containing the resolution and speed of the end point [9]. Hwang presented an optimization design based on genetic algorithm, including three performance index [10]. Liu proposed a modular robot design, considering the workspace, strange isotropic and GCI performance metrics [11]. Oetomo etc. presented a mechanical arm design method based on interval search [12].

In this paper, an optimized RCM mechanism is proposed, turning the double parallelogram mechanism into a single parallelogram mechanism, under the request of the surgical operation. Except for the improved structure, in order to make the mechanism have a better performance, an objective optimization function is presented, based on the condition number index and the workspace. The optimization results are drawn in the paper.

2 Structure Scheme

To meet the motion constrains for the MIS application, a compact 4DOF RCM mechanism is proposed. The RCM mechanism is composed of a single parallelogram mechanism and a steel belt. To comprehend this method, the double parallelogram mechanism, as the most widely used mechanism in MIS robot, could be used as an object. It is a planar RCM mechanism, formed by two parallelogram linkages together, shown in Figure 2. The end link of the mechanism, could be a fixed point during the movement, which become the RCM point.

A revolute joint is added in the mechanism whose axis passes through the RCM point, driving the whole mechanism out of the plane. The RCM point could be seen as an intersection point of two axes of the two movable planes. However, it has many rods and high requests for the installation accuracy.

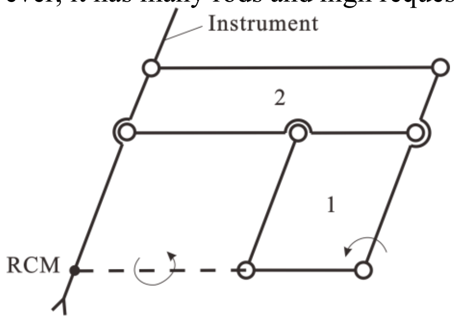

Figure 2: The double parallelogram mechanism

The single parallelogram mechanism just replace one motion plane by using the constraints of the steel belt, as shown in Figure 3. The mechanism could maintain its original geometric constraints, smoothly completes the movement in the MIS robot. Through the constraints of the steel, the relations between the rotations of the each revolute joint could remain the same, meeting the geometry requests in the parallelogram motion.

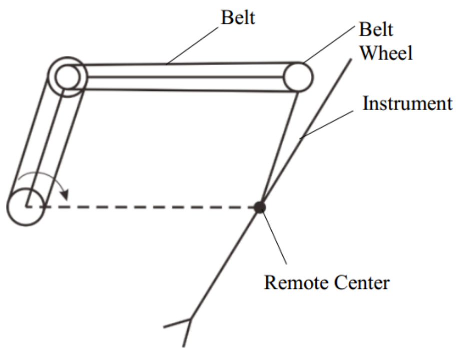

Figure 3: The single parallelogram mechanism

The kinematic structure of the RCM mechanism is shown in Figure 4. The joint 1 is a passive joint, it could be used to adjust the position of the active joints before the operation. Active revolute joint 2 controls the motion of the single parallelogram mechanism during the operation. Joint 3 provides the gyroscopic moment for the RCM mechanism,

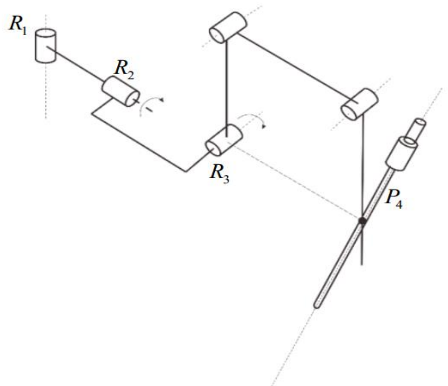

Figure 4: The kinematic structure of the mechanism

while the prismatic joint 4 could provide the straight line movement for the surgical instruments along the rod direction.

3 Kinetic analysis

The kinematic model is shown in Figure 5, several coordinate systems for kinematic analysis can be built. The transform matrix can be expressed as below. α is the angle between the first passive joints and the horizontal plane, and β is the equipment and rotary joint angle.

Position vector parameters present as follows:

$$\begin{cases} p_x = d_3 s_3 (c_1 c_2 + s_1 s_2 \sin\alpha) - s_1 c_3 \cos\alpha - d_1 s_1 \cos\alpha \\ p_y = d_3 s_3 (s_1 c_2 - c_1 s_2 \sin\alpha) + c_1 c_3 \cos q_1 + d_1 c_1 \cos\alpha \\ p_z = -d_1 \sin\alpha - d_3 (c_3 \sin\alpha + s_2 s_3 \cos\alpha) \end{cases} \quad (1)$$

where $s_i = \sin(\theta_i)$, $c_i = \cos(\theta_i)$, $i = 1, 2, 3$.

Considering the equation of motion of the robots as,

$$\boldsymbol{x} = \boldsymbol{x}(\boldsymbol{q}) \quad (2)$$

The output velocity $\dot{\boldsymbol{x}}$ is related to the input joint velocity $\dot{\boldsymbol{q}}$ by

$$\dot{\boldsymbol{x}} = \boldsymbol{J}(\boldsymbol{q})(\dot{\boldsymbol{q}}) \quad (3)$$

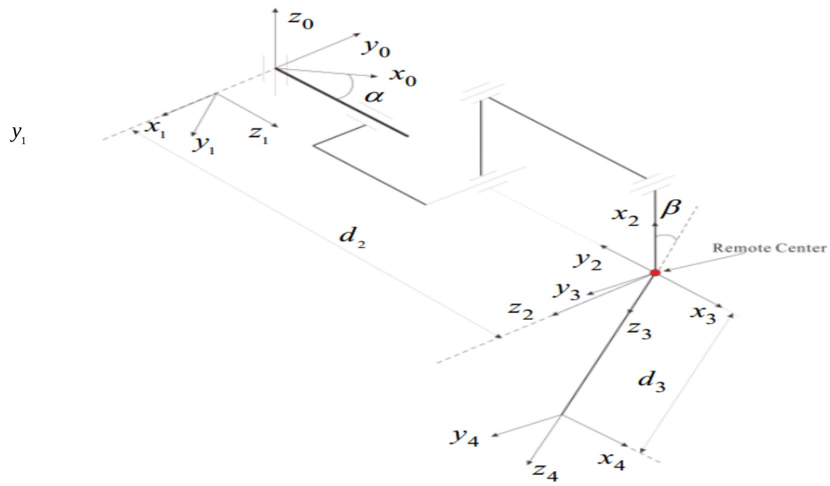

Figure 5: The kinematic model of the mechanism

The linear operator J is the Jacobian matrix, could be written as

$$\begin{bmatrix} \boldsymbol{v} \\ \boldsymbol{w} \end{bmatrix} = \boldsymbol{J}\dot{\boldsymbol{\theta}} = \begin{bmatrix} J_{l1} & J_{l2} & \cdots & J_{ln} \\ J_{a1} & J_{a2} & \cdots & J_{l1} \end{bmatrix} \begin{bmatrix} \dot{q}_1 \\ \dot{q}_2 \\ \vdots \\ \dot{q}_n \end{bmatrix} \tag{4}$$

The resolve method of the Jacobian matrix is vector product method, based on the motion coordinate concept. The result is shown in Equation (5).

$$J(q) = \begin{bmatrix} z_1 \times ({}^0_1R\,{}^1P_4) & z_2 \times ({}^0_2R\,{}^2P_4) & z_3 \times ({}^0_3R\,{}^3P_4) & z_4 \\ z_1 & z_2 & z_3 & 0 \end{bmatrix} \tag{5}$$

where ${}^iP_n$ represents the end of origin of coordinates relative to the coordinate system $\{i\}$ of position vector expressed in the base coordinate system $\{o\}$, where ${}^iP_n{}^0 = {}^0_iR\,{}^iP_n$.

z_i is the axis unit vector in z axis of coordinate system $\{i\}$ expressed in base coordinate system O, where $\boldsymbol{z}_i = {}^0_i\boldsymbol{R}\boldsymbol{e}_3$,

$$\boldsymbol{e}_3 = \begin{bmatrix} 0 & 0 & 1 \end{bmatrix}^T,\ {}^0_i\boldsymbol{R} = {}^0\boldsymbol{R}_1\,{}^1\boldsymbol{R}_2 \cdots {}^{n-1}\boldsymbol{R}_n,\ i = 1,2\cdots n .$$

4 The optimization model

In order to improve the performance of the mechanism, an optimization method is presented. The performance and the workspace analysis are analysed, which contributes to the optimization of the mechanism parameters. Structure parameters are optimized with the object function, which combines the condition number index and the workspace index.

4.1 Kinematic Performance

The mechanism operability is a suitable index for evaluating the kinetic performance of a manipulator, based on the condition number k. The value of the condition number k should be small.

$$k = \|\mathbf{J}\|\|\mathbf{J}^{-1}\| \tag{6}$$

The range of k is $[1,+\infty)$, when $k=1$, institution is in isotropic state, while $k \to \infty$, the mechanism is in singular configuration. The value of the condition number k should be small. Condition number has the following relationship with singular value, that is,

$$k = \frac{\sigma_{\max}(J)}{\sigma_{\min}(J)} \tag{7}$$

It is necessary to consider that the condition number k is a local performance measurement and it varies when the configuration of the mechanism changes. So Global condition number was then proposed by integrating the local dexterity over the workplace. That is,

$$\eta = \frac{A}{B} \tag{8}$$

Where $A = \int_W (1/k)dw$, $B = \int_W dw$, and W is the workspace of the mechanism, the range of η is $[0,1)$. A better overall performance is achieved when η is maximized.

Figure 6 and Figure 7 shows the variation of η, θ_2 and d_3, It can be seen that η decrease with the increase of θ_2 or d_3. The distribution of η is a plane symmetrical graph, which means the effects of θ_2 and d_3 on η are identical.

It can be seen that the mechanism performances well when θ_2 in the range of $[-45°, 45°]$. And with the increase of d_3, the η decrease. So a reasonable range of d_3 is set to $[15, 300]$.

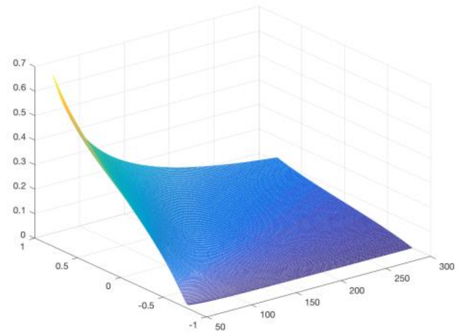

Figure 6: The distribution of η, θ_2 and d_3

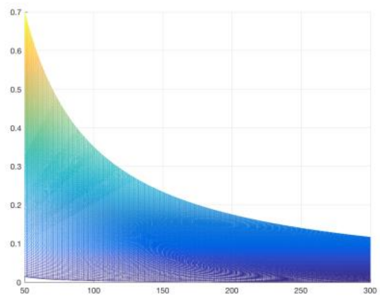

Figure 7: The projection of the distribution of η and d_3

4.2 Workplace Analysis

Through the kinematic analysis of the mechanism, we could know that the variables $d_2, d_3, \theta_1, \theta_2, \theta_3$ have influence on the motion of the end. According to the need in the process of operation and the structure properties of the instrument itself, the mechanism should swing respectively in two direction with the fixed RCM point, in the angle of 90° and 60°. Therefore, three revolute joint vary in the range of $\theta_1 \in (-45°, 45°)$, $\theta_2 \in (-60°, 60°)$, $\theta_3 \in (-60°, 60°)$. In order to analyze the impact of d_2, d_3 to the workspace, taking 6 different data groups of d_2, d_3, comparing the workspace of the end of the instruments. The Monte Carlo method is used to draw its working space, as shown in Figure 8.

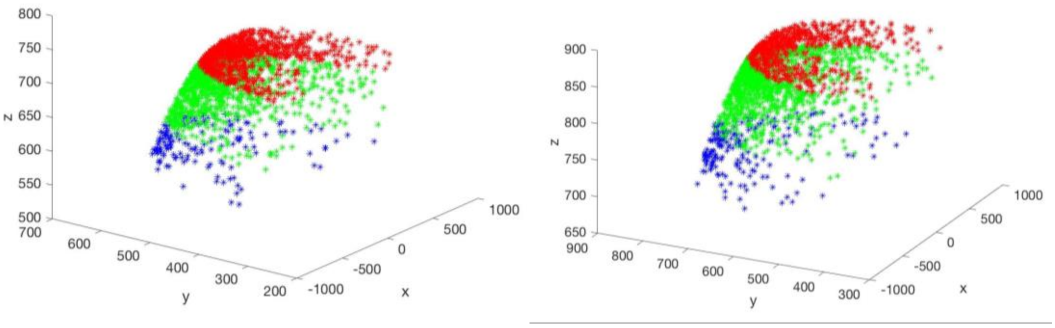

(a) $d_2 = 800,\ d_3 = 200$ (b) $d_2 = 1000,\ d_3 = 200$

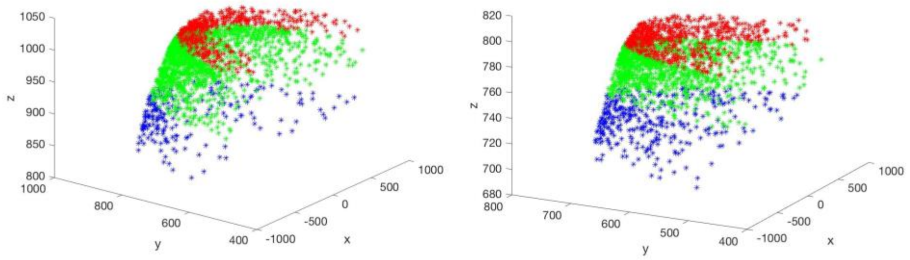

(c) $d_2 = 1200,\ d_3 = 200$ (d) $d_2 = 1000,\ d_3 = 100$

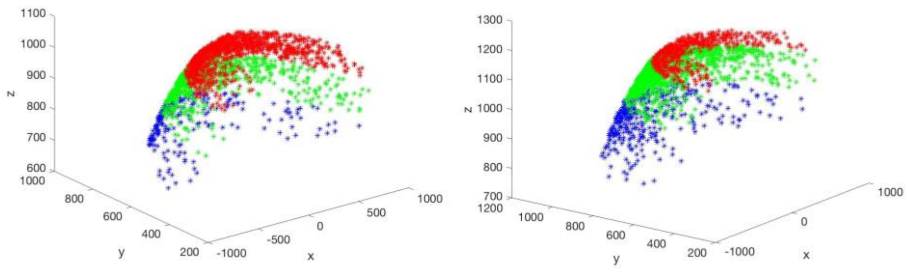

(e) $d_2 = 1000,\ d_3 = 400$ (f) $d_2 = 1200,\ d_3 = 400$

Figure 8: The variations of the workspace through different parameters of d_2 and d_3 (unit: mm)

It could be seen in Figure 8, when $d_3 = 200$ mm, with the increasing of d_2, the effective space increases along the z axial direction. When $d_2 = 1000$ mm, with the increase of d_3, the effective space increases along the y axial direction. The workspace rely on the coordination of d_2 and d_3.

4.3 Optimization Design

The optimization model is constructed with two objective function, that is, the condition number index η and the working space V, which contribute to the performance of the mechanism movement.

$$f = w_1\eta + w_2 V \qquad (9)$$

Where w_1, w_2 are the weight coefficients. Considering the influence of maneuverability and operating space on the actual operation, taking $w_1 = 0.5$, $w_2 = 0.5$. Considering with the increase of η, the institution tends to be more isotropic, and the maneuverability becomes better. The bigger of V, the greater of the effective working space. Selcted f as the optimization objective function, that is,

$$\max f = w_1\eta + w_2 V \qquad (10)$$

In the optimization model, the condition number index η and the working space V have relationship with the rob parameters d_2, d_3 and the rotation angel $\theta_1, \theta_2, \theta_3$. During the mechanism optimazation, taking the rob length and the angle of rotation parameters as the main consideration. Because θ_1 is related to preoperative placement optimization model, so ignore the influnce of θ_1, choosing $d_2, d_3, \theta_2, \theta_3$ as design variables. The constraint conditions are $800 \le d_2 \le 1500$,

$15 \le d_3 \le 300$, $45^\circ \le \theta_{2\max} \le 90^\circ$, $-90^\circ \le \theta_{2\min} \le -45^\circ$, $45^\circ \le \theta_{3\max} \le 90^\circ$, $-90^\circ \le \theta_{3\min} \le -45^\circ$,the units of d_2 and d_3 are millimeters.

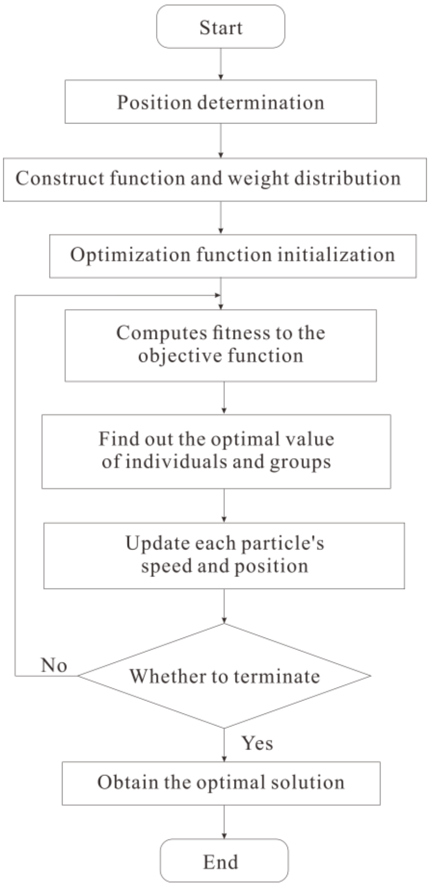

Figure 9: The flow chart of PSO

Particle swarm optimization (PSO) is a population-based swarm intelligence algorithm [13], with fast speed and high precision. Setting the population of size n, then each particle is expressed as $x_i = (d_{2i}, d_{3i}, \theta_{2\max i}, \theta_{2\min i}, \theta_{3\max i}, \theta_{3\min i})$, and the scope of i is $i = 1, 2, \cdots n$. The searching space of the particles is six dimensional space, corresponding speed for each particle $(V_{d_{2i}}, V_{d_{3i}}, V_{\theta_{2\max i}}, V_{\theta_{2\min i}}, V_{\theta_{3\max i}}, V_{\theta_{3\min i}})$.When each particle search in the space, there are two factors needed to be considered, one is the history optimal values of one particle, the other one is the optimal value of all particles. We can obtain better parameter after taking round-off numbers, the optimization results are listed in Table 1.

Table 1: Optimization parameters of the mechanism

θ_2	θ_3	d_2	d_3
$\left[-64^\circ, 69^\circ\right]$	$\left[-72^\circ, 79^\circ\right]$	992mm	253mm

After the optimization, compare the effective workspace with ordinary situation. It could be seen in Figure 10, the effective working space increase with better performance. After the optimization, the mechanism has good maneuverability and enough operation space, and it can meet the requirements in the process of operation.

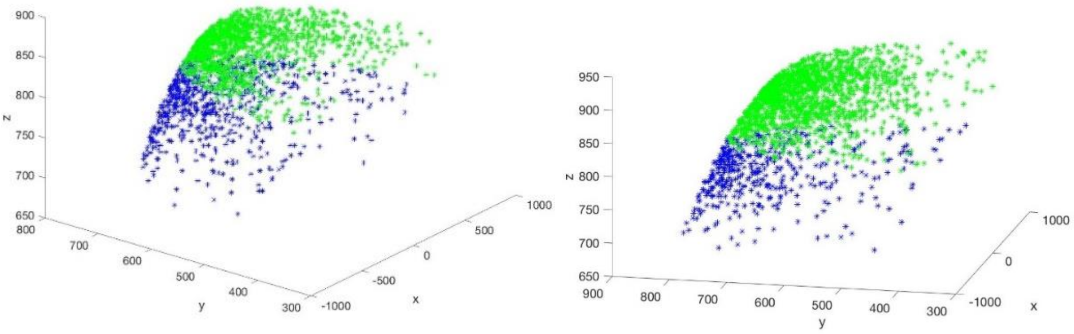

(a) Before optimization (b) After optimization

Figure 10: The operation space of the mechanism

Based on the dimensional parameters obtained above, a prototype of the robot is shown in Figure 11. The translational range of the active prismatic joint is 300mm in this design. The scheme shows that a proposed robot can be used to assist the surgeon to manipulate the instrument in a MIS.

Figure 11: A prototype of the proposed RCM mechanism

5 Conclusion

A new single parallelogram mechanism of RCM is proposed in this paper. Based on the kinetic model of the mechanism, the performance and the workspace are analyzed, which contributes to the optimization of the mechanism parameters. Structure parameters are optimized with the object function, which combines the condition number index and the workspace index, then the results working well.

Acknowledgements

This paper was supported by grants from National Natural Science Foundation of China (No. 61403108).And the work was carried out at State Key Laboratory of Robotics and System, Harbin Institute of Technology. The authors would like to thank all the supports and helps for this research.

References

[1] Diana C. W, Mitchell J. H. Lum, et al. “The RAVEN: Design and Validation of a Telesurgery

System", The International Journal of Robotics Research. 28(9), pp.1183-1197, (2009).

[2] Li, J. M., Xing, Y., Liang, K. "Kinematic Design of a Novel Spatial Remote Center-of-Motion Mechanism for Minimally Invasive Surgical Robot", Journal of Medical Devices, Vol. 9, 1-8, (2015).

[3] Guthart, G. S., Salisbury, J. K., Jr. "The IntuitiveTM Telesurgery System: Overview and Application", IEEE International Conference on Robotics and Automation, San Francisco, CA, Apr. 24–28, pp. 618–62, (2000).

[4] Gosselin, C., and Angeles, J. "A Global Performance Index for the Kinematic Optimization of Robotic Manipulators", ASME J. Mech. Des., 113(3), pp. 220–226, (1991).

[5] Yoshikawa, T. "Analysis and Control of Robot Manipulators With Redundancy", Robotics Research The First International Symposium, MIT Press, Cambridge, MA, pp. 735–747, (1984).

[6] Yoshikawa, T. "Manipulability of Robotic Mechanisms", Int. J. Robot.Res., 4(2), pp. 3–9, (1985).

[7] Klein, C. A. "Use of Redundancy in the Design of Robotic Systems", Robotics Research The Second International Symposium, MIT Press, Cambridge, MA, pp. 207–214, (1985).

[8] Stocco, L, Salcudean, S, and Sassani, F. "Matrix Normalization for Optimal Robot Design", Proc. IEEE International Conference on Robotics and Automation, Leuven, Belgium, Vol. 2, pp. 1346–1351, (1998).

[9] Lan Peng, Liu Manlan, Lu Nian-li. "Optimal design of a novel high speed and high precision 3-DOF manipulator", Proceedings of the 2005 IEEE International Conference on Mechatronics. Taipei, Taiwan, IEEE, pp. 689-69, (2005).

[10] Hwang Y K, Yoon J W, Ryu J H. "The optimum design of a 6-DOF parallel manipulator with large orientation workspace", SICE-ICASE International Joint Conference, Bustan, Korea, SICE-ICASE, pp. 18-2, (2006).

[11] Liu Hai tao, Huang T, Mei Jian ping. "Kinematic design of a 5-DOF hybrid robot with large workspace/limb-stroke ratio", Journal of Mechanical Design, 129(5), pp. 530-537, (2007).

[12] Oeromo D, Daney D, Merlet J P. "Design strategy of serial manipulators with certified constraint satisfaction", IEE Transactions on Robotics, 25(1), pp. 1-11, (2009).

[13] Dos Santos Coelho L. "Gaussian quantum-behaved particle swarm optimization approaches for constrained engineering design problems", Expert Systems with Applications, 37(2), pp.1676-1683, (2010).